System Identification and model comparison of a Tension Leg Platform for Floating Offshore Wind Turbines

Hansen, Thomas; Jørgensen, Maria A. B.; Tran, Van Roy; Jessen, Kasper; N. Soltani, Mohsen

Published in:
2019 24th International Conference on Methods and Models in Automation and Robotics, MMAR 2019

DOI (link to publication from Publisher):
10.1109/MMAR.2019.8864710

Publication date:
2019

Document Version
Early version, also known as pre-print

System Identification and model comparison of a Tension Leg Platform for Floating Offshore Wind Turbines

1st Thomas Hansen
Department of Energy Technology
Aalborg University
Esbjerg, Denmark
th15@student.aau.dk

2nd Maria A. B. Jørgensen
Department of Energy Technology
Aalborg University
Esbjerg, Denmark
mjorge15@student.aau.dk

3rd Van Roy Tran
Department of Energy Technology
Aalborg University
Esbjerg, Denmark
vtran15@student.aau.dk

4th Kasper Jessen
Department of Energy Technology
Aalborg University
Esbjerg, Denmark
kje@et.aau.dk

5th Mohsen N. Soltani
Department of Energy Technology
Aalborg University
Esbjerg, Denmark
sms@et.aau.dk

***Abstract*—This paper will focus on using system identification on experimental data for building a mathematical model for the platform of a floating offshore wind turbine and analyzing the behavior of the structure. The floating offshore wind turbine examined in this paper uses a scaled tension leg platform as its foundation and the wind turbine is a 1:35 scaled model of the 5 MW NREL offshore wind turbine.**
The mathematical model of the platform will describe the displacement of the TLP in surge when affected by an irregular wave series generated from a scaled Pierson-Moskowitz wave spectrum. To obtain such a mathematical model, an examination of the displacement of the platform due to the hydrodynamic loads will be conducted on the foundation of the floating offshore wind turbine. The height of the waves and the displacement of the floating offshore wind turbines will be measured by resistive wave gauges and OptiTrack cameras, respectively, at the offshore laboratory at Aalborg University Esbjerg. System identification is used on the data obtained from the experiments, to build multiple mathematical models with different model structures, in order to find the most appropriate model structure. It is concluded from the analysis of the different mathematical models, that the Autoregressive Moving Average and Extra input model structure is the most accurate model at describing the dynamics of the platform of a floating offshore wind turbine. The model is valid for a specific operating range of Pierson-Moskowitz waves generated with a wind speed corresponding to 2 meters per seconds.

***Index Terms*—System identification, SI, floating offshore wind turbines, FOWT, TLP, Pierson-Moskowitz, scaled-model**

I. Introduction

FLOATING offshore wind turbines are increasingly becoming a more relevant topic for extending the buildable area for wind turbines offshore. Floating Offshore Wind Turbines (FOWT) are, however, still in their exploratory stage, since an in depth understanding of the loads and dynamic behavior is still being developed due to the complexity of floating offshore structures. The modeling of the dynamics of floating offshore wind turbines is usually conducted by non-linear mathematical models. These models are complex and computationally expensive. Previous work on a scaled floating offshore wind turbine in [1] and [2] has developed these numerical models for the presented scaled floating offshore wind turbine structure. The use of System Identification (SI) can ease the complexity and computational time of the model. In recent years, SI has become an increasingly popular tool for determining a mathematical model of a dynamical system. The modeling complexity of modern systems is increasing, therefore, SI is becoming more attractive as a mathematical model can be build from experimental data of the input and output of the system.

Throughout this paper, the fundamentals of SI will not be explored, as there already exist publications on the subject such as [3] and [4]. Some papers focus more on different methods for SI such as [5], which explains how SI can be used to model a non-linear black-box model of a system. As described by [4], "SI is a broad topic, with different ways of interpreting and describing the theory, but the goal is, however, always to define a descriptive mathematical model of a specific system."
The contribution of this paper to the field of SI is to determine a system identified model, which describes the dynamic behavior of a Tension Leg Platform (TLP) used for a FOWT. The theory and methodology for SI in this paper are based on the contribution to the field by [6].
The use of SI for FOWT are still limited, and only a few studies have been conducted. Similar work at Aalborg University Esbjerg (AAUE) in [7], investigated the possibility to use SI on the same experimental setup as this paper. The

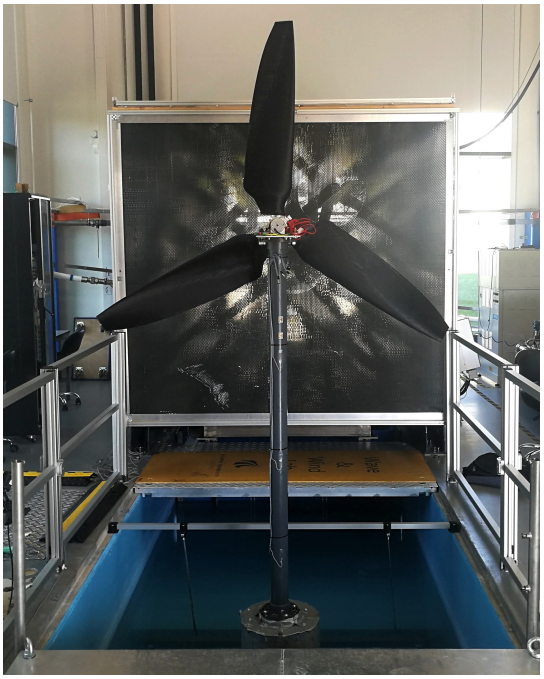

Fig. 1. Test facility of the FOWT in front of wind generator at AAUE

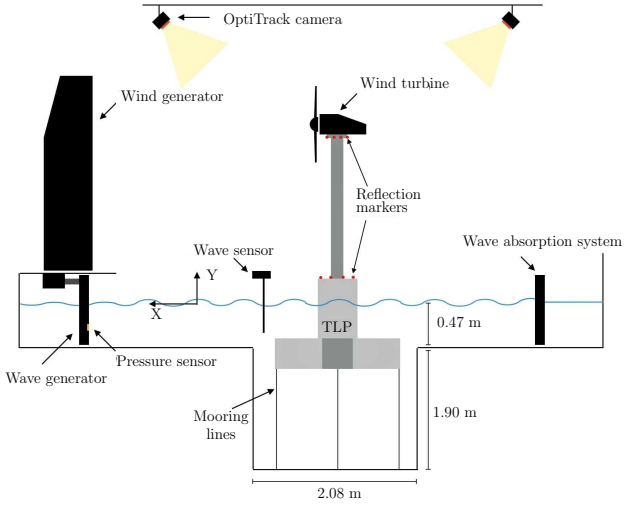

Fig. 2. Illustration of the offshore facility [7]

results obtained in [7] is comparable with the results obtained in this research, however, the model coefficients obtained in this paper is different.

This paper focuses on a scaled FOWT consisting of a scaled TLP design based on [8], and a scaled version of the National Renewable Energy Laboratory's (NREL) 5 MW offshore wind turbine [9]. The 1:35 Froude scaled model has been designed and developed in the report [10] and is denoted as AAUE-TLP. The scaled FOWT setup is located at Aalborg University Esbjerg's (AAUE) Offshore Laboratory.

A representation of the FOWT, as well as the setup at the laboratory, can be seen in figure 1 and figure 2.

To obtain a mathematical model of the FOWT, data have been obtained through experiments. These data include information about the input and output of the system, which in this case is the wave height and displacement of the FOWT in the surge direction, respectively. Initially, the experimental data will be used to develop non-parametric models in the frequency domain which will be used for further analysis and validation of the parametric models. These parametric model will be developed based on the experimental data, through an iterative optimization process, where different quantitative qualities of the models will be compared. These different qualities include fit, auto- and cross-correlation, and frequency response. Finally, the validated non-parametric model will be used to determine the accuracy of the parametric models' behavior in the frequency domain.

The paper is organized as follows: The experiment conduction can be found in section II, the identified models are represented in section III, the validation and comparison can be found in section IV, and finally, the conclusion will be found in section V.

II. Experiment Conduction

To obtain the necessary data for developing a mathematical model of the FOWT, multiple experiments have been conducted with irregular waves determined by a specific wave spectrum. The time series based on the wave spectrum is calculated in the program AwaSys [11] which also controls the wave generator. Equation (1) is used to define the Pierson-Moskowitz (PM) spectrum in AwaSys.

$$S_{PM}(f) = \frac{\alpha g^2}{(2\pi)^4} f^{-5} \exp\left(-\frac{0.74 g^4}{(2\pi f U_{19.5})^4}\right) \tag{1}$$

Where α is a constant of 0.0081, g is the gravitational constant, and $U_{19.5}$ is the wind speed at the height of 19.5 m above the surface of the sea [12]. For these experiments, $U_{19.5}$ is set to 2 m/s, corresponding to a wind speed of 12 m/s for the full-scale model. At a wind speed of 12 m/s, the 5 MW NREL wind turbine has reached its maximum power region. The wind speed has been scaled using Froude scaling, with a scaling factor of $\sqrt{35}$.

The PM spectrum has been generated with a time period of 300 s and a sampling frequency of 50 Hz. The wave heights are measured, with the use of three resistive probes placed in front of the TLP through a first order lowpass filter with a 16 kHz cutoff frequency.

The variance spectrum for the waves measured in the experiments can be seen in figure 3, it should be noted the the wave height in each experiment is based on the average wave height from the three resistive probes. The variance spectrum is the average spectrum based on multiple experiments, statistically, the average wave spectrum is more accurate, than a single spectrum from each experiment [13]. Figure 3 also contains the theoretical PM spectrum used by AwaSys to generate the irregular waves.

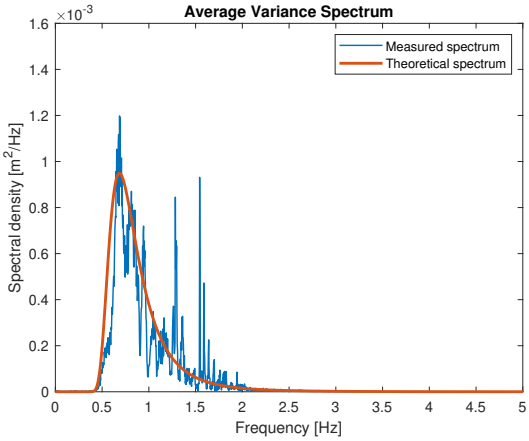

Fig. 3. The average variance spectrum of the waves in the experiments and the theoretical variance spectrum

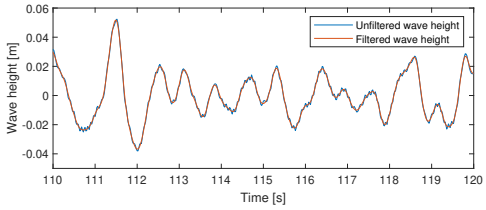

Fig. 4. Experimental time series data of the wave height with and without the Butterworth filter

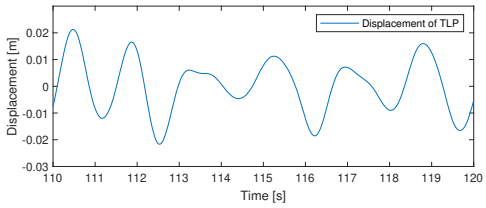

Fig. 5. Experimental time series data of the surge displacement of the TLP

From figure 3 it can be seen, that the experimental calculated wave spectrum correspond to the requested theoretical PM spectrum. However, there are two frequencies where peaks are measured. The two peaks are thought to be caused by wave reflections from the TLP and the wave basin. The displacement of the FOWT caused by the irregular waves is recorded by using the motion capturing software Motive from OptiTrack. Motive uses multiple cameras to capture the motion of the TLP by tracking reflection markers placed on the TLP. From the recording, the displacement in space can then be calculated. Motive is calibrated to have a sampling frequency of 50 Hz, and accuracy of $\pm$ 0.56 mm. Only the displacement in the surge direction will be used in the SI process.

During the analysis of the measured wave height, some unwanted noise was detected. The noise was removed by applying a 3rd order Butterworth filter with a cutoff frequency of 4 Hz.
A part of the experimental time series for the filtered and unfiltered wave height and the surge displacement of the TLP can be seen in figure 4 and 5.

For the SI process, the experimentally obtained time series data of the wave height and displacement of the TLP in surge was combined into several IDData object in MATLAB and split up into two groups. The IDData object encapsulates the input/output data along with their properties. The two groups consist of identification data and validation data, and these have been used for the subsequent analysis, identification and validation. Each IDData object has a duration of 280 s, and only consist of steady state data as the transition periods in the start and end of the recording have been removed.

III. SI MODELS

The system identification has been divided into two parts. The first part is to identify the behavior of the system using a non-parametric model. The second part is to determine a parametric model, which is able to simulate and predict the behavior of the system accurately. The parametric model will be compared to the non-parametric model for further model validation.

In the identification of a non-parametric model, both spectral analysis (SPA) and Empirical Transfer Function Estimate (ETFE) was examined. According to the results presented in figure 6, the SPA was found to be insufficient in explaining the dynamics of the system. However, the ETFE was able to accurately represent the behavior of the FOWT over a wide range of frequencies. This has been further validated by comparing the response from the ETFE with experimentally determined localized gains in the frequency domain. These localized gains are represented as validation points in figure 6, where the ETFE models and the validation points are superimposed. The validation points have been determined by applying regular waves of specific frequencies to the FOWT. The frequencies were chosen to verify the important dynamics, such as the natural frequency and cutoff response of the FOWT. Due to limitations in the experimental setup, it has not been possible to verify the ETFE model in frequencies higher than 6 rad/s.

Next, a parametric model is to be determined. The dynamic behavior of the final model should be comparable to the response of the ETFE. It should also have good prediction capabilities in the time domain as well as having good performance in a correlation analysis.
Since SI is an iterative process, a logic loop with a focus on the fit percentage of a simulation with infinite prediction horizon. The coefficients and fit percentage for the infinite prediction horizon can be seen in table I. In the further examination of the different models from table I, the models' frequency response in comparison with the ETFE presented in figure 7, shows a different result than that of the fit percentage. As an example the Output-Error (OE) and

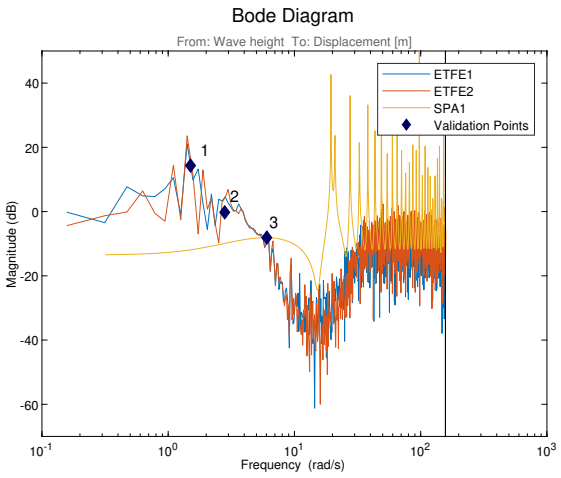

Fig. 6. Bode diagram of ETFE and SPA with validated points determined experimentally

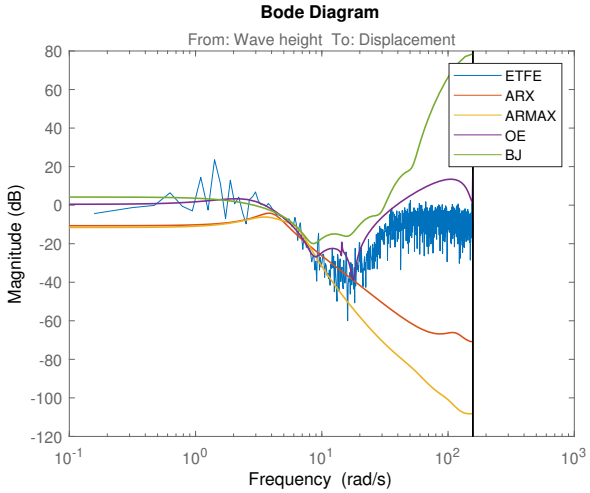

Fig. 7. Frequency response of the different parametric models in comparison to the ETFE

TABLE I
COEFFICIENTS AND CORRESPONDING FIT OF THE MODEL STRUCTURES DETERMINED BY ITERATION IN LOGIC LOOP

Model	A	B	C	D	F	K	Fit [%]
ARX	5	1				0	43.1
ARMAX	9	1	3			10	-13.03
OE		10			7	10	-11.09
BJ		9	6	10	1	0	55.83

Box-Jenkins (BJ) model have a vastly different fit percentage, however, their frequency response is very similar. Based on this difference a more in-depth comparison should be conducted when determining a model, which can sufficiently describe the behavior of the FOWT in both the time- and frequency domain. It should be noted that responses at frequencies greater than 6 rad/s, will not be considered in the analysis, due to the maximum validation frequency previously discussed.

The resulting coefficients found during the logic loop will be used as an initial guess in the further analysis. This further analysis applies a more manual approach focusing on extracting as much information from the data as possible. In this analysis, the parameters used in the comparison are the auto- and crosscorrelation between the output and input, as well as the frequency response of the models and lastly the fit percentage.

During the analysis ARX, OE, and BJ were found to be insufficient model structures, since none of them were able to be sufficiently explained by the validation points seen in figure 6, especially the TLP's natural frequency. This insufficient behavior was also apparent in their performance for auto- and crosscorrelation. The ARMAX model structure showed the most promising results according to its frequency response and performance in auto- and crosscorrelation.

As a result, three proposed ARMAX models found manually

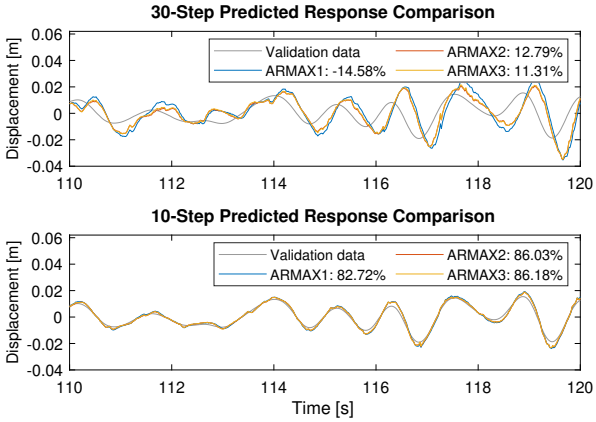

Fig. 8. 10- and 30-step ahead prediction for the different ARMAX models

have been analyzed in further details. The coefficients of these models can be seen in table II.

One of the requirements for the final model states that it should have good prediction capabilities in the time domain. As a parameter, the number of steps ahead which a model can predict determines along with the fit percentage how good the specific model is at simulating the behavior of the structure over time. Based on the sampling frequency and the performance of the models a step ahead prediction of 10- and 30-steps have been chosen. The prediction of the three ARMAX models is shown in figure 8.

The large difference between the two predicted responses in figure 8 shows the diminishing capabilities of the models prediction at higher step ahead predictions.

By analyzing the residuals of the different ARMAX models for the 10-step ahead prediction, it is possible to determine the model's degree of explanation according to the validation data. It is desired that the prediction error (PE) is contained within a specific confidence interval to resembles white noise. The

TABLE II
MANUALLY CHOSEN COEFFICIENTS FOR ARMAX MODEL ANALYSIS

	a	b	c	k
ARMAX1	9	7	3	10
ARMAX2	7	4	4	10
ARMAX3	7	4	3	10

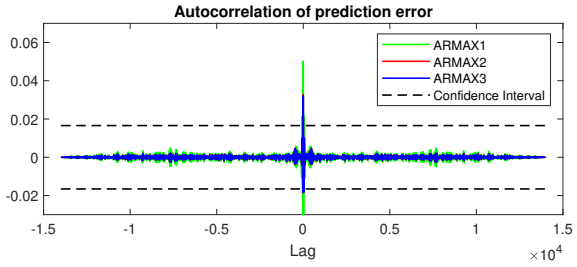

Fig. 9. Autocorrelation of PE for the different ARMAX models

confidence interval is determined by a significance level of 5 % in a Z-distribution as shown in equation 2

$$C.I. = \pm 1.96 \frac{1}{\sqrt{n}} \tag{2}$$

Where n is the number of samples in the dataset.
By analyzing the autocorrelation of the PE, it is possible to determine whether the PE has any unwanted correlation with itself. The autocorrelation for the three ARMAX models can be seen in figure 9, which shows no autocorrelation for any of the three models.

Due to the similar coefficients for ARMAX2 and ARMAX3, only a negligible difference between their autocorrelation is present and can therefore not be distinguished in neither figure 9 and figure 10. Besides from the autocorrelation of the PE, the crosscorrelation between the PE for both the input and output are just as important to analyze. By analyzing the crosscorrelation, the amount of extractable information from the data can be determined. In figure 10, the crosscorrelation between the PE for both input and output can be seen.

The three ARMAX models show sufficient performance in the crosscorrelation between the PE and output. The amount of points outside the confidence interval does not exceed the expected limit of 5% of the sample size.
The crosscorrelation between the PE and input does, however, exceed the limit and shows some unwanted correlation. This unwanted behavior decreases the amount of information extracted from the supplied data.

The results of the auto- and cross-correlations are also apparent in the frequency response of the models shown in figure 11 along with the ETFE model. A clear difference is present between the three models, especially in the low-frequency range gain, and at the natural frequency gain of the TLP.

The final chosen model is ARMAX3, based on its overall performance and especially its resemblance to the frequency response of the ETFE.

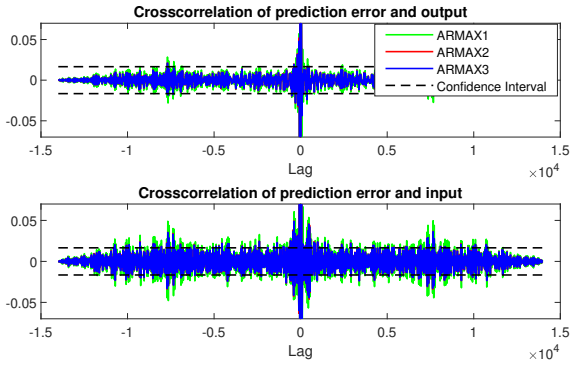

Fig. 10. Crosscorrelation between PE for both input and output

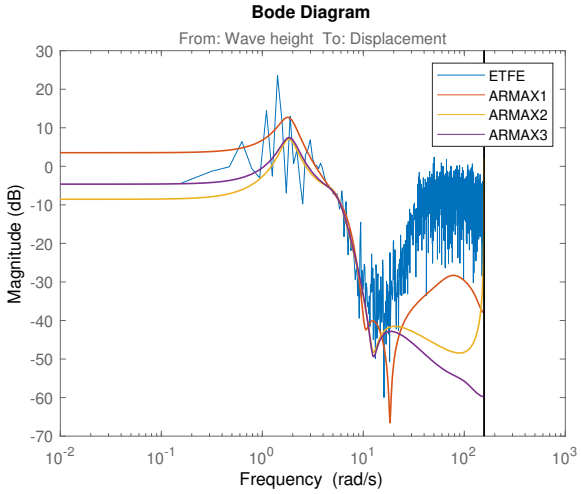

Fig. 11. Comparison of the frequency response for the ARMAX models and the frequency response of the ETFE

IV. VALIDATION

Further analysis of the final model is needed to determine its validity, and for this purpose, a secondary validation dataset is used. The data has been gathered with the same parameters as the previous validation data, due to the randomness of the wave generation, the two validation datasets are non-identical.

First, the model is used to simulate the 10- and 30-step ahead prediction, as shown in figure 12, and by comparing these results to figure 8, an improved fit percentage is obtained. This improvement shows the model's prediction capability is largely affected by the supplied experimental data. From these results, it can be determined that a higher uncertainty in fit percentage is present at a higher step ahead predictions.
Further analysis of the auto- and crosscorrelation of the model's PE has also been conducted. Figure 13 shows these correlations, and a small improvement across the figures is apparent compared to ARMAX3 in figure 9 and 10.

As in the previous correlation analysis, the tendencies of the correlations are similar, meaning the model is able to

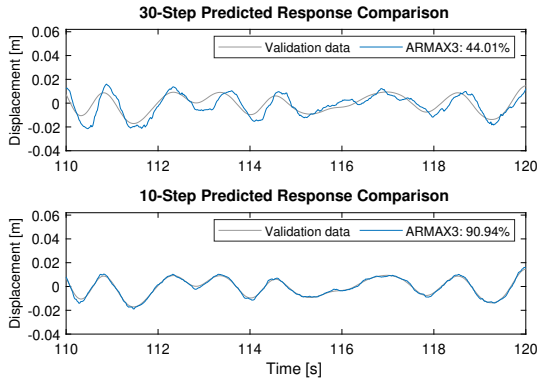

Fig. 12. 10- and 30-step ahead prediction for the final ARMAX model

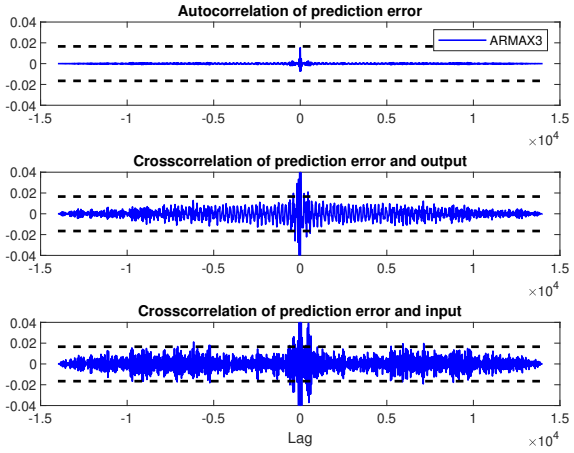

Fig. 13. Auto- and crosscorrelation of PE and both output and input data

reproduce similar results for different independent datasets, within its specified operating region.

The final ARMAX3 model structure can be written as

$$y = \frac{B(q)}{A(q)}u(t) + \frac{C(q)}{A(q)}y(t) \tag{3}$$

Where the A, B, C coefficients are given as

$$A(q) = 1 - 4.232q^{-1} + 6.977q^{-2} - 5.634q^{-3} + 2.478q^{-4} - 0.9222q^{-5} + 0.4489q^{-6} - 0.1165q^{-7}$$

$$B(q) = 0.002745q^{-10} - 0.008243q^{-11} + 0.008423q^{-12} - 0.00293q^{-13}$$

$$C(q) = 1 - 2.689q^{-1} + 2.514q^{-2} - 0.8242q^{-3}$$

V. Conclusion

By using data obtained from experiments specifically designed for SI, it was found that a mathematical model for the FOWT was able to be devised.

In conclusion, a linear system identified model capable of predicting the behavior of the FOWT at a wind speed of 2 m/s was found. The final model shows a good fit in the 10-step ahead prediction, but its 30-step ahead prediction does, however, vary depending on, which validation data was given to the model. It shows good performance for its auto- and crosscorrelation, and its frequency response is similar to the estimation determined by the validated ETFE.

For future research, it is relevant to investigate a wider operating range for such model, as well as looking into the effect of wind disturbance and how such disturbance could be implemented into a system identified model.

References

[1] S. M. Mortensen, K. Laugesen, J. K. Jensen, K. Jessen, and M. Soltani, "Experimental verification of the hydro-elastic model of a scaled floating offshore wind turbine," in *2018 IEEE Conference on Control Technology and Applications (CCTA)*, Aug 2018, pp. 1623–1630.

[2] K. Jessen, K. Laugesen, S. M. Mortensen, J. K. Jensen, and M. N. Soltani, "Experimental validation of aero-hydro-servo-elastic models of a scaled floating offshore wind turbine," *Applied Sciences*, vol. 9, no. 6, 2019. [Online]. Available: http://www.mdpi.com/2076-3417/9/6/1244

[3] G. P. Rao and H. Unbehaun, "Indentification of continous-time systems," *IEE Proc.- Control Theory Appl.*, vol. 153, no. 2, 2006.

[4] L. Fu and P. Li, "The research survey of system identification method," *IEE Computer Society*, vol. 978-0-7695-5011-4/13, 2013.

[5] J. Sjöberg, Q. Zhang, L. Ljung, A. Benveniste, B. Delyon, P.-Y. Glorennec, H. Hjalmarsson, and A. Juditsky, "Nonlinear black-box modeling in system identification: a unified overview," *Automatica*, vol. 31, no. 12, pp. 1691 – 1724, 1995, trends in System Identification. [Online]. Available: http://www.sciencedirect.com/science/article/pii/0005109895001208

[6] L. Ljung, *System Identification - Theory for the User*. University of Sweden, 1987.

[7] C. Lindquist, P. Nielsen, R. Pedersen, and M. Soltani, "Experimental modelling of a floating offshore wind turbine," in *2018 23rd International Conference on Methods Models in Automation Robotics (MMAR)*, Aug 2018, pp. 327–332.

[8] E. E. Bachynski, "Design and dynamic analysis of tension leg platform wind turbines," Ph.D. dissertation, Norges teknisk-naturvitenskapelige universitet, 2014.

[9] J. Jonkman, S. Butterfield, W. Musial, and G. Scott, "Definition of a 5-mw reference wind turbine for offshore system development," National Renewable Energy Laboratory, Tech. Rep., 2009.

[10] J. K. Jensen, K. Jessen, K. Laugesen, and S. M. Mortensen, "Aero-hydro-servo-elastic modelling and control of a scaled floating offshore wind turbine on a tension leg platform including experimental validation," Aalborg University, Master thesis, 2018.

[11] T. L. Andersen, "Awasys 7," https://www.hydrosoft.civil.aau.dk/awasys/.

[12] A. Chadwick, J. Morfelt, and M. Borthwick, *Hydraulics in civil and enviromental engineering*, 5th ed. CRC Press, 2013.

[13] M. Casas-Prat, "Overview of ocean wave statistics," Ph.D. dissertation, 07 2008.